Conjugated vs Nonconjugated Bridges: Heterogeneous Electron Transfer Dynamics of Osmium Polypyridyl Monolayers

ARTICLE *in* LANGMUIR · AUGUST 2000

Impact Factor: 4.46 · DOI: 10.1021/la000718s

6 AUTHORS, INCLUDING:

Egbert Figgemeier
3M Deutschland
34 PUBLICATIONS **787** CITATIONS
SEE PROFILE

Johan Hjelm
Technical University of Denmark
64 PUBLICATIONS **1,157** CITATIONS
SEE PROFILE

Johannes G Vos
Dublin City University
306 PUBLICATIONS **7,146** CITATIONS
SEE PROFILE

Conjugated vs Nonconjugated Bridges: Heterogeneous Electron Transfer Dynamics of Osmium Polypyridyl Monolayers

Robert J. Forster,*,† Egbert Figgemeier,†,‡ Paul Loughman,† Anthea Lees,† Johan Hjelm,§ and Johannes G. Vos†

National Centre for Sensor Research, School of Chemical Sciences, Dublin City University, Dublin 9, Ireland, and Department of Physical Chemistry, Uppsala University, Box 532, S-75121 Uppsala, Sweden

Received May 6, 2000

Introduction

The production of "molecular wires" that promote fast heterogeneous electron transfer between a remote redox center and a metal surface is important for high-speed molecular electronics applications, e.g., molecule-based computing. One notable strategy in this area is to use conjugated rather than aliphatic bridges to achieve faster electron-transfer rates. For example, conjugated molecules of [1,1′:4′,1″-terphenyl]-4-methanethiol (TP) have been embedded in self-assembled monolayers of insulating *n*-alkanethiols and the conductivity of single molecules measured.[1] Also, Creager and co-workers[2] recently probed the electron transfer rates for ferrocene groups attached to gold electrodes via conjugated oligo(phenylethynyl) bridges of variable length. Significantly, they found that the extrapolated rate constants at short distances were nearly the same for conjugated and aliphatic bridges. Moreover, for short electron-transfer distances, the observed rates were consistent with those expected for an adiabatic electron transfer suggesting strong electronic coupling between the redox centers and the electrode. In this context, experiments with self-assembled monolayers consisting of osmium 2,2′6′,2″-terpyridine complexes attached to an electrode surface by 4′-(3-pyridyl)-2,2′:6′,2″-terpyridine were performed recently. The heterogeneous electron-transfer rate constants for this system do not show a substantial increase compared to those found for comparable aliphatic bridges.[3] However, directly comparing heterogeneous electron transfer rate constants will provide an insight into the strength of electronic coupling only if the free energy of activation is identical for conjugated and nonconjugated bridges. For example, switching from a nonconjugated to a conjugated bridging ligand may alter the structure of the monolayer making the local dielectric content and hence outer sphere reorganization energies different in the two cases.

We report here on the effect of using a conjugated, *trans*-1,2-bis(4-pyridyl)ethylene, bpe, vs a nonconjugated bridge, 1,2-bis(pyridyl)ethane, p2p, on the heterogeneous electron-transfer rate constants for $[Os(bpy)_2Cl]^+$ moieties attached to the surface of platinum microelectrodes (Chart 1). Cyclic voltammetry has been used to measure the rate of heterogeneous electron transfer for monolayers of $[Os(bpy)_2(bpe)Cl]^+$ using scan rates up to 10 000 V s^{-1}. These data have been compared with previous reports[4−6] on the nonconjugated bridge, 1,2-bis(pyridyl)ethane. To determine whether differences in electronic coupling or the free energy of activation are responsible for the observed differences in $k°$, the complete voltammograms have been fitted using an overlap integral approach based on the Marcus relation.

Chart 1

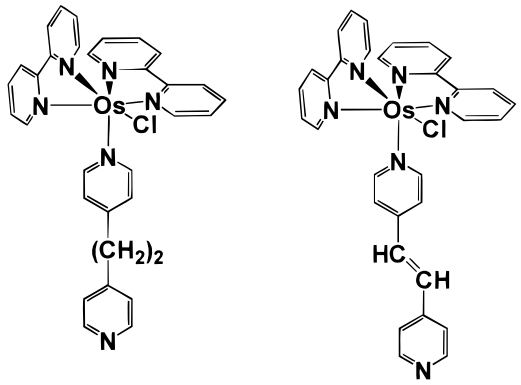

p2p: 1,2-bis(4-pyridyl)ethane bpe : *trans*-1,2-bis(4-pyridyl)ethylene

Experimental Section

Reagents and Synthesis. The complex was synthesized using methods similar to those published previously.[7] $[Os(bpy)_2(bpe)Cl](PF_6)_2$ was synthesized by first refluxing $[Os(bpy)_2Cl_2]$ (0.22 g, 3.5×10^{-4} mol) in dry methanol (10 cm^3) until completely dissolved. *trans*-1,2Bis(4-pyridyl)ethylene) (0.07 g, 3.8×10^{-4} mol) was added over 1 h, and the resulting solution was refluxed for a further 12 h. After this period the reaction mixture was cooled and added dropwise to a concentrated aqueous solution of NH_4PF_6. Elemental analysis, NMR, HPLC, and UV−vis spectroscopy all indicate that the compound is obtained in the form $[Os(bpy)_2(bpeH)Cl](PF_6)_3$, where the free pyridine group is protonated. That the unbound pyridine moiety of the 1,2-bis-(4-pyridyl)ethylene ligand is protonated is not unexpected since the synthesis was carried out in dry methanol. This protonation does not persist in aqueous media, and the complex is capable of forming spontaneously adsorbed monolayers.

Electrochemistry. Cyclic voltammetry was performed using a CH Instruments model 660 electrochemical workstation and a conventional three-electrode cell with a BAS Ag/AgCl electrode as reference. Microelectrodes were fabricated from platinum and gold microwires (Goodfellow Metals Ltd.) of radii between 1 and 25 μm by sealing them into soft glass using a procedure described previously.[5] The microdisk electrodes were prepared by mechanical polishing and voltammetric cycling in dilute acid in order to create a clean polycrystalline surface of known microscopic area. Typically the surface roughness was between 1.3 and 1.6. RC cell time constants were between 0.03 and 3 μs, depending on the electrode radius and the supporting electrolyte concentration.

Preparation of Monolayers. Spontaneously adsorbed monolayers were typically formed by placing a freshly prepared electrode in a 2 mM solution of the complex dissolved in aqueous acetone (50:50 v/v) containing 0.1 M $LiClO_4$ as supporting electrolyte. The electrode was poised at 0.1 V vs Ag/AgCl during the 30 min deposition cycle. Prior to deposition, all solutions

† Dublin City University.

‡ Current address: Institute for Inorganic Chemistry, University of Basel, Spitalstrasse 51, 4056 Basel, Switzerland.

§ Uppsala University.

(1) Ishida, T.; Mizutani, W.; Akiba, U.; Umemura, K.; Inoue, A.; Choi, N.; Fujihira, M.; Tokumoto, H. *J. Phys. Chem. B* **1999**, *103*, 1686.
(2) Weber, K. S.; Creager, S. E. *J. Electroanal. Chem.* **1998**, *458*, 17.
(3) Figgemeier, E.; Zimmermann Y.; Houscroft, C. E.; Constable, E. C. To be submitted for publication.
(4) Acevedo, D.; Abruña, H. D. *J. Phys. Chem.* **1991**, *95*, 9590.
(5) Forster, R. J.; Faulkner, L. R. *J. Am. Chem. Soc.* **1994**, *116*, 5444.
(6) Forster, R. J.; Faulkner, L. R. *J. Am. Chem. Soc.* **1994**, *116*, 5453.
(7) Forster, R. J. *Inorg. Chem.* **1996,** *35*, 3394.

10.1021/la000718s CCC: $19.00
Published on Web 08/31/2000

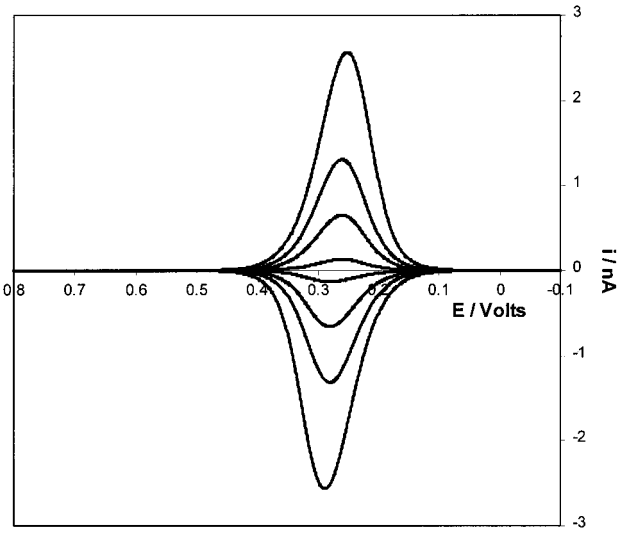

Figure 1. Background-corrected cyclic voltammograms for a spontaneously adsorbed $[Os(bpy)_2(bpe)Cl]^+$ monolayer on a 25 μm radius platinum microdisk electrode. The supporting electrolyte is aqueous 0.1 M $LiClO_4$. The scan rate from top to bottom is 2, 1, 0.5, and 0.1 V s^{-1}. Cathodic currents are up, and anodic currents are down.

were degassed for at least 15 min using nitrogen, and a blanket of nitrogen was maintained over the solution during all experiments.

Results and Discussion

General Electrochemical Properties. Figure 1 shows a typical background corrected cyclic voltammogram for a spontaneously adsorbed monolayer of $[Os(bpy)_2(bpe)Cl]^+$ on a 25 μm radius platinum microdisk as the scan rate, v, is systematically varied from 0.1 to 2 V s^{-1}. The formal potential for the osmium monolayer is 0.28 V, which agrees closely with that found for this complex by Abruña[8,9] and with values reported for monolayers assembled from the complex $[Os(bpy)_2(p2p)Cl]^+$, where p2p is the corresponding nonconjugated bridge 1,2-bis(4-pyridyl)ethane)[5,8] ($E^{\circ\prime} = 0.31$ V).

The limiting surface coverage of the complex at equilibrium is $(7.0 \pm 0.5) \times 10^{-11}$ mol cm^{-2} and does not increase further by increasing the concentration of the complex in solution or the deposition time. This saturation coverage is smaller than that found by Acevedo and Abruña[4,8] for monolayers of the same complex but lies within the range measured previously for related systems.[8,11,13] The full width at half-maximum, fwhm, is between 100 and 120 mV at slow scan rates (<5 V s^{-1}), which is slightly higher than the ideal case of 90.6 mV for a one-electron transfer. This broadening is consistent with weak repulsive interactions between the adsorbates most likely arising from their cationic character.[10,11]

Electron-Transfer Dynamics. The standard heterogeneous electron-transfer rate constant, $k°$, depends on both a frequency factor and a Franck−Condon barrier[12−14]

$$k° = A_{et} \exp(-\Delta G^{\ddagger}/RT) \quad (1)$$

where A_{et} is the pre-exponential factor (equal to the product of Γ_n the nuclear tunneling factor, κ_{el} the electronic transmission coefficient, and v_n the nuclear frequency factor) and $\Delta G^{\ddagger}$ is the electrochemical free energy of activation.[15]

One approach to decoupling these two contributions is to use classical temperature-resolved measurements of $k°$ to measure the free energy of activation, $\Delta G^{\ddagger}$, allowing A_{et} to be determined. In this way, information about the strength of electronic coupling can be obtained.[6,16,17] A second method involves measuring electron-transfer rate constants at a single temperature over a broad range of reaction driving forces. For example, Finklea and Hanshew,[18] have assembled a model describing through-space electron tunneling which provides a good description of electron tunneling in monolayers of this kind.[5] In this model, the cathodic rate constant is given by integral over energy (E) of three functions: (a) the Fermi function for the metal $n(E)$, (b) a Gaussian distribution of energy levels for acceptor states in the monolayer $D_{Ox}(E)$, and (c) a probability factor describing electron tunneling at a given energy, $P(E)$.

$$k_{Ox}(\eta) = A\int_{-\infty}^{\infty} D_{Ox}(E)\, n(E)\, P(E)\, d\epsilon \quad (2)$$

The zero point of energy is defined as the Fermi level of the metal at the particular overpotential of interest. The Fermi function describes the distribution of occupied states within the metal and is defined by

$$n(E) = \left(\frac{1}{1 + \exp[(\epsilon - \epsilon_F)/kT]}\right) \quad (3)$$

where k_B is the Boltzmann constant. The density of acceptor states is derived from the Marcus theory[19,20] and is represented by eq 4

$$D_{Ox}(E) = \exp\left[-\frac{(E + \eta - \lambda)^2}{4k\lambda T}\right] \quad (4)$$

where λ is the reorganization energy. The probability of direct elastic tunneling[21,22] through a trapezoidal energy barrier of height E_B can be approximated by eq 5

$$P(E) = (E_B - E + e\eta/2) \exp(-\beta d) \quad (5)$$

where E_B is the average barrier height at zero overpotential (taken here as 2.0 eV) and d is the electron-transfer distance.

Chidsey,[23] Creager,[24] and Murray[25] have modeled nonadiabatic heterogeneous electron transfer for long-chain alkanethiol monolayers using an expression similar

(8) Acevedo, D.; Bretz, R. L.; Tirado, J. D.; Abruña, H. D. *Langmuir* **1994**, *10*, 1300.
(9) Acevedo, D.; Bretz, R. L.; Tirado, J. D.; Abruña, H. D. *Langmuir* **1994**, *10*, 1971.
(10) Brown, A. P.; Anson, F. C. *Anal. Chem.* **1977**, *49*, 1589.
(11) Laviron, E. *J. Electroanal. Chem.* **1974**, *52*, 395.
(12) Bagchi, G. *Annu. Rev. Chem.* **1989**, *40*, 115.
(13) Sutin, N. *Acc. Chem. Res.* **1982**, *15*, 275.
(14) Barr, S. W.; Guyer, K. L.; Li, T. T.-T.; Liu, H. Y.; Weaver, M. J. *J. Electrochem. Soc.* **1984**, *131*, 1626.
(15) Sutin, N. Brunschwig, B. S. *ACS Symp. Ser.* **1982**, *No. 198*, 105.
(16) Forster, R. J.; Vos, J. G.; Keyes, T. E. *Analyst* (*Cambridge, U.K.*) **1998**, *123*, 1905.
(17) Forster, R. J.; O'Kelly, J. P. *J. Phys. Chem.* **1996**, *100*, 3695.
(18) Finklea, H. O.; Hanshew, D. D. *J. Am. Chem. Soc.* **1992**, *114*, 3173.
(19) Marcus, R. A. *J. Chem. Phys.* **1956**, 24, 966.
(20) Marcus, R. A. *J. Phys. Chem.* **1963**, *67*, 853.
(21) Schmickler, W. *J. Electroanal. Chem.* **1977**, *82*, 65.
(22) Bockris, J. O'M.; Khan, S. U. M. *Quantum Electrochemistry*; Plenum Press: New York, 1979; Chapter 8
(23) Chidsey, C. E. D. *Science* **1991**, *251*, 919.
(24) Weber, K.; Creager, S. E. *Anal. Chem.* **1994**, *66*, 3164.
(25) Tender, L.; Carter, M. T.; Murray, R. W. *Anal. Chem.* **1994**, *66*, 3173.

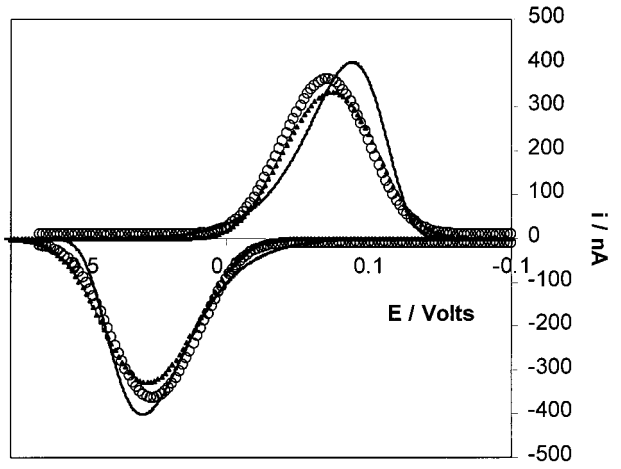

Figure 2. Cyclic voltammograms for a spontaneously adsorbed $[Os(bpy)_2(bpe)Cl]^+$ monolayer on a 25 μm radius platinum microdisk electrode at a scan rate of 6000 V s^{-1}. The solid line denotes experimental data, while ○ and ▲ denote the best-fit theoretical responses generated using the Finklea and Chidsey models, respectively. Both theoretical responses correspond to a $k°$ of 9.4×10^3 s^{-1} and a $\Delta G^‡$ of 11.4 kJ mol^{-1}. The supporting electrolyte is aqueous 0.1 M $LiClO_4$.

to eq 2 except that the energy-dependent prefactor in the tunneling probability expression is excluded.

The current for the reaction of an immobilized redox center following first-order kinetics is[25]

$$i_F = nFA(k_{Ox}(\eta)\,\Gamma_{Red,\eta} - k_{Red}(\eta)\Gamma_{Ox,\eta}) \qquad (6)$$

where $\Gamma_{Red,\eta}$ and $\Gamma_{Ox,\eta}$ are the instantaneous surface coverages of the oxidized and reduced species and $k_{Ox}(\eta)$ and $k_{Red}(\eta)$ are the reaction rate constants and are given by eq 2 with or without a tunneling probability function. In using eq 6 to model the voltammetric response, the electron-transfer distance, d, is taken as 10 Å leaving only two freely adjustable parameters, $k°$ and $\Delta G^‡$ ($=\lambda/4$). We have used both of these models in a finite difference simulation to determine $k°$ and $\Delta G^‡$. To achieve this objective, we have used the Nelder and Mead Simplex[26] algorithm to find the values of $k°$ and $\Delta G^‡$ that minimize the sum square residuals between the theoretical and experimental currents observed in anodic branches of the linear sweep voltammograms.

Figure 2 shows the experimental background corrected cyclic voltammogram for a dense $[Os(bpy)_2(bpe)Cl]^+$ monolayer deposited on a 5 μm radius platinum microelectrode where the scan rate is 6000 V s^{-1}. The overall cell resistance in this experiment is approximately 18 kΩ. Given that the peak current in Figure 2 is approximately 400 nA, the ohmic loss will be less than 8 mV, which is negligible compared with the observed ΔE_p of approximately 310 mV. Figure 2 illustrates the best fits obtained from eqs 2−6 for models that include and exclude through-space tunneling through a trapezoidal barrier. In both cases the residual sum of squares between theory and experiment was minimized *only* for the oxidative branch and then the best fit estimates of $k°$ and $\Delta G^‡$ obtained were used to predict the cathodic branch of the voltammogram. For both models, the optimum $k°$ was $(9.4 \pm 0.9) \times 10^3$ s^{-1} and $\Delta G^‡$ was 11.4 ± 0.8 kJ mol^{-1}.

Figure 2 shows that excellent agreement is observed between the experimental and theoretical anodic peak potentials and both peak currents. Moreover, there is general agreement between the theoretical and experimental currents along the full anodic branch. However, poorer agreement is observed for the cathodic branch, which may arise from oxidation state dependent electronic coupling or, more likely, differences in the reorganization energy caused by changes in the monolayer's solvation as it is oxidized.[27] Figure 2 reveals that while the quality of the fit obtained using the two models is broadly comparable, the peak currents predicted by Finklea's through-space tunneling model more closely match the experimental values. That these voltammograms are bet described by a through-space tunneling model agrees with previous investigations[5] where a value of 1.6 ± 0.2 $Å^{-1}$ was obtained[5] for the distant dependent tunneling parameter, β. A through-space rather than through-bond mechanism is somewhat surprising given the aromatic character of the *trans*-1,2-bis(4-pyridyl)ethylene bridge. However, it is important to note that the electron-transfer distance examined here, 10 Å, is considerably shorter than that traditionally explored using alkanethiol self-assembled monolayers, 20−30 Å. Quantum mechanical spillover of the metal electron density beyond the electrode/monolayer interface, and the delocalized character of the electron density on the electrode, may be relatively more important for these short bridging ligands. Furthermore, electric field effects may influence the electron-transfer dynamics because the length of the bridge and the double layer thickness are comparable.[17]

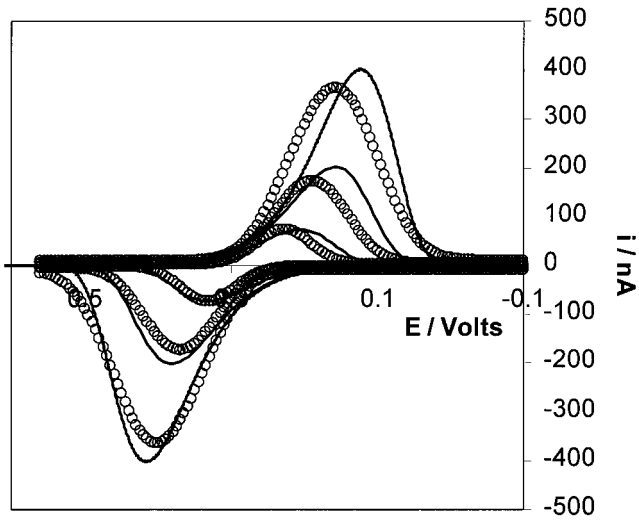

Figure 3. Experimental (—) and theoretical (○) voltammograms generated using the through-space tunneling model due to Finklea, for a spontaneously adsorbed $[Os(bpy)_2(bpe)Cl]^+$ monolayer on a 25 μm radius platinum microdisk electrode. From top to bottom, the scan rates are 6000, 3000, and 1000 V s^{-1}. In all cases, the theoretical responses were generated using a $k°$ of 9.4×10^3 s^{-1} and a $\Delta G^‡$ of 11.4 kJ mol^{-1}.

An important test of the reliability of the standard heterogeneous electron-transfer rate constants obtained by fitting the cyclic voltammograms is to investigate the scan rate dependence. In this way, an insight into the dispersion in the kinetics can be obtained. Figure 3 shows the fits obtained at scan rates of 1000, 3000, and 6000 V s^{-1}. In each case the same fitting parameters for the Finklea model, i.e., a $k°$ of 9.4×10^3 s^{-1} and a $\Delta G^‡$ of 11.4 kJ mol^{-1}, were used. For each scan rate, there is satisfactory agreement between the theoretical model and the experimental currents of the anodic branch of the voltammogram. That the experimental responses at different

(26) Ebert, K.; Ederer, H.; Isenhour, T. L. *Computer Applications in Chemistry*: *An Introduction for PC Users*; VCH Publishers: New York, 1989.

(27) Hupp, J. T.; Weaver, M. J. *J. Phys. Chem.* **1984**, *88*, 6128.

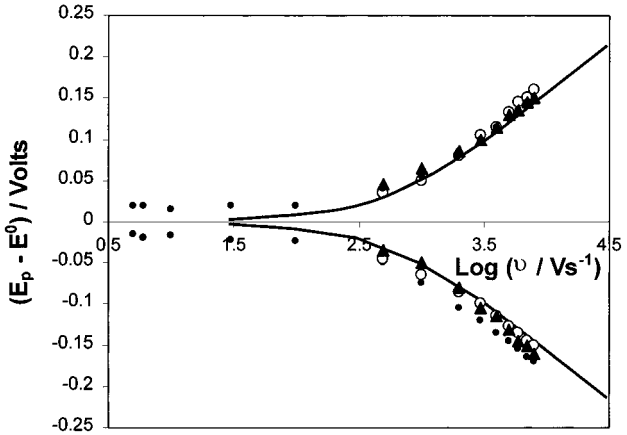

Figure 4. Plot of ($E_p - E°$) vs log(sweep rate) for a spontaneously adsorbed monolayer of $[Os(bpy)_2(bpe)Cl]^+$. The experimental data are denoted by ● while ○ and ▲ denote best-fit theoretical responses generated using the models assembled by Finklea and Chidsey, respectively. Both theoretical responses correspond to a $k°$ of 9.4×10^3 s^{-1} and a $\Delta G^‡$ of 11.4 kJ mol^{-1}. The solid line denotes the prediction of the Butler−Volmer theory ($\alpha = 0.5$, $k° = 9.4 \times 10^3$ s^{-1}). The supporting electrolyte is 0.1 M $NaClO_4$.

time scales are accurately modeled using the same two parameters indicates that the heterogeneous electron transfer rate constants are all similar for individual adsorbates corresponding to indistinguishable microenvironments and electron transfer distances. This nearly ideal behavior contrasts with that observed for ferrocene alkanethiol monolayers[23,24] where it is difficult to achieve satisfactory agreement between theory and experiment over the entire voltammogram due to oxidation state dependent lateral interactions.

Given the difficulties of accurately removing background charging currents from experimental voltammograms, an alternative procedure is to probe the dependence of the anodic and cathodic peaks potentials, $E_{p,a}$ and $E_{p,c}$, on the voltammetric scan rate. Figure 4 illustrates the dependence of the peak-to-peak separation, ΔE_p, on the voltammetric scan rate for $8000 \geq \upsilon \geq 5$ V s^{-1}. For scan rates up to approximately 100 V s^{-1} ΔE_p is insensitive to the scan rate before increasing significantly. There are two important processes that could contribute to the observed response: first, ohmic loss due to the higher current density at higher scan rate;[28] second, slow heterogeneous electron transfer across the electrode/monolayer interface. As discussed previously, in experiments of this kind, the *iR* drop is kept below 5 mV by carefully selecting the radius of the microelectrode. Thus, while high-quality data can be obtained from a monolayer coated 25 μm radius microdisk for $\upsilon < 100$ V s^{-1}, for higher scan rates 1 μm radius electrodes are used.[29] Moreover, the same slope is observed in Figure 4 if the experiments are repeated in more conducting solutions that contain a higher concentration of supporting electrolyte. This observation also indicates that secondary processes, e.g., ohmic loss, or the dynamics of ion pairing, do not contribute significantly to the observed response. The behavior illustrated in Figure 4 is consistent with the dynamics of heterogeneous electron-transfer influencing the voltammetric response at high scan rates.

Figure 4 shows the peak potentials predicted by the models assembled by Chidsey[23] and Finklea[18] using values of $k°$ and $\Delta G^‡$ of 9.4×10^3 s^{-1} and 11.4 kJ mol^{-1}, respectively. In common with the analysis of the complete voltammograms, there is good agreement between theory and experiment for the anodic branch but somewhat poorer agreement for the cathodic data. As discussed by Creager,[24] the peak potentials are rather insensitive to the reorganization energy allowing accurate values of $k°$ to be obtained essentially independently of λ. Figure 4 also shows the predictions of the classical Butler−Volmer theory[28] which tends to overestimate the apparent heterogeneous electron-transfer rate constant.

Table 1. Rate Constants, Free Energies of Activation, and Pre-exponential Factors for the $Os^{2+/3+}$ Redox Reaction Occurring within $[Os(bpy)_2(L)Cl]^+$ Monolayers Where L Is *trans*-1,2-Bis(4-pyridyl)ethylene (bpe) or 1,2-Bis(4-pyridyl)ethane (p2p)[a]

bridging ligand	$10^{-3}k°/s^{-1}$	$\Delta G^‡$/kJ mol^{-1}	$10^{-6}A_{et}/s^{-1}$
bpe	9.4 ± 0.9	11.4 ± 0.8	0.9 ± 0.3
p2p	305 ± 26	8.7 ± 1.2	11.1 ± 0.5

[a] Supporting electrolyte is 0.1 M aqueous $LiClO_4$.

As described previously,[5,8,30] the voltammetric response of $[Os(bpy)_2(p2p)Cl]^+$ monolayers is generally similar to that presented above for the bpe-bridged systems. We have modeled the voltammetric response for the p2p-bridged system and found values $(3.00 \pm 0.26) \times 10^5$ s^{-1} and 8.7 ± 1.2 kJ mol^{-1} for $k°$ and $\Delta G^‡$, respectively. This $k°$ is indistinguishable from that determined previously using potential step chronoamperometry conducted on a microsecond time scale.[30] Therefore, it appears that despite the bpe bridge being conjugated the heterogeneous electron transfer rate constant is approximately a factor of 30 smaller than that found for the aliphatic bridge, 1,2-bis-(4-pyridyl)ethane. However, as discussed above, in trying to elucidate the effect of changes in bridge structure, e.g., conjugation, it is important to determine the pre-exponential factors since these are sensitive to the degree of electronic coupling across the bridge.[7] Table 1 contains the free energies of activation for both the bpe and p2p systems. While both the $\Delta G^‡$ values agree with that predicted by the Marcus relation for outer sphere reorganization[31] to within 20%, $\Delta G^‡$ is smaller for the p2p system. This difference in the free energy of activation most likely corresponds to a different monolayer structure in the two circumstances and would correspond to more nonpolar environment within the p2p-bridged monolayer.

We have used the values of $k°$ and $\Delta G^‡$ in conjunction with eq 1 to estimate pre-exponential factors for both the bpe- and p2p-bridged monolayers. The data are summarized in Table 1. These data reveal that the prefactors are approximately 6 orders of magnitude smaller than those expected for an adiabatic electron transfer, i.e., one involving strong coupling between the localized redox states of the monolayer and delocalized metallic states of the electrode. However, the most significant result contained in Table 1 is that the pre-exponential factor is approximately an order of magnitude higher for the p2p than for the bpe bridge indicating that the redox center and electrode are more strongly coupled for the aliphatic system.

This result is consistent with the through-space tunneling mechanism in that the less rigid p2p bridge probably has sufficient flexibility to reduce the electron-transfer distance below the value of 10 Å expected on the basis of a rigid-rod model. It is important to note that unlike a

(28) Bard, A. J.; Faulkner, L. R. *Electrochemical Methods, Fundamentals and Applications*; John Wiley & Sons: New York, 1980.
(29) Forster, R. J. *Phys. Chem. Chem. Phys.* **1999**, *1*, 1543.
(30) Forster, R. J.; Faulkner, L. R. *Anal. Chem.* **1995**, *67*, 1232.
(31) Weaver, M. J. *Chem. Rev.* **1992**, *92*, 463.

through-space pathway, the electron-transfer distance for through-bond tunneling mechanisms is independent of the monolayer's conformation. Therefore, the *decrease* in heterogeneous electron-transfer rate constant observed here on going from a nonconjugated to a conjugated bridge is not expected for a through-bond tunneling mechanism.

Conclusions

Monolayers of $[Os(bpy)_2(bpe)Cl]^+$ have been formed and their electrochemical properties investigated. We have modeled the voltammetric response observed at high scan rates where heterogeneous electron transfer across the metal/monolayer interface influences the experimental response. Somewhat surprisingly, despite the conjugated bridge and short electron-transfer distance, the voltammetric response is best modeled as a through-space tunneling process. The standard heterogeneous electron-transfer rate constant, $k°$, for the conjugated bridge is 9.4 $\times$ 10^4 s^{-1} which is approximately a factor of 30 *smaller* than that observed for a longer, aliphatic bridge, 1,2-bis-(4-pyridinyl)ethane. Modeling the complete voltammogram allows the contributions from electronic coupling and free energy of activation to be decoupled. This analysis reveals free energies of activation of 8.7 $\pm$ 1.2 and 11.4 $\pm$ 0.8 kJ mol^{-1} for the bpe and p2p bridges, respectively. That the voltammetric response is best described using a through-space tunneling model and both the standard heterogeneous electron-transfer rate constants and pre-exponential factors are larger for the nonconjugated ligand suggest that heterogeneous electron-transfer proceeds via a through-space tunneling mechanism.

Acknowledgment. The authors thank the EC TMR Programme (Contract Number CT96-0076) for financial assistance.

LA000718S